Biosensors and Bioelectronics 138 (2019) 111302

Contents lists available at ScienceDirect

Biosensors and Bioelectronics

journal homepage: www.elsevier.com/locate/bios

A supersensitive MSPQC bacterium sensor based on 16S rRNA and "DNA-RNA switch"

Ye Feng[a], Xiaoqing Zhang[a,b], Lingling Su[a], Yilin Zhang[a], Fengjiao He[a,*]

[a] State Key Laboratory of Chemo/Biosensing and Chemometrics, College of Chemistry and Chemical Engineering, Hunan University, Changsha, 410082, China
[b] School of Pharmacy, Hunan University of Chinese Medicine, Changsha, 410208, China

ARTICLE INFO

Keywords:
16S ribosomal-RNA
Bacterium
E. coli
MSPQC sensor
DNA-RNA switch

ABSTRACT

The early detection of bacterium plays a significant role in addressing serious public health issues. In this paper, a supersensitive multichannel series piezoelectric quartz crystal (MSPQC) sensor of bacterium based on 16S rRNA and "DNA-RNA switch" was constructed. The fragment in specific region of 16S rRNA was used as the biomarker of bacterium to ensure high specificity and to achieve the accurate judgment of microbial vitality. "DNA-RNA switch" was designed to conduct two electrodes by switching insulated "gene-link" into conductive "silver-link", which achieved the super-sensitivity of MSPQC to bacteria. To demonstrate the feasibility of this strategy, a proof-of-concept method for *Escherichia coli* (*E. coli*) assay was designed. The detection limit was down to 2 cfu/mL. *Staphylococcus aureus, Salmonella enteritidis, Listeria innocua* and *Pseudomonas aeruginosa* did not interfere with the detection results. Proposed method was highly sensitive, and specific for bacterium detection, which might find widely use in early detection of bacterium in the field of public safety monitoring and clinical diagnosis.

1. Introduction

Bacterium has a vital role in resolving global crisis such as environmental pollution, food security, and epidemic disease (Zhang et al., 2018; Zhou et al., 2016). Therefore, efficient bacterium detection techniques have attracted extensive attention in the world (Chen et al., 2018). To date, the detection methods of bacterium can be classified into culture and non-culture methods. The culture method is of low cost, high accuracy and can achieve the detection of microbial viability and validity. However, the lengthy time (Gayathri et al., 2016), laborious operation (Zhang et al., 2016), and most importantly, the limitation in detecting viable but non-culturable (VBNC) microbes which caused relapse in clinic diagnosis (Yu et al., 2017) have become the driving force to the development of non-culture methods. Non-culture methods are based on biomarkers (e.g. antibodies (Gayathri et al., 2016), nucleic acids (Sun et al., 2016) etc.,) combined with signal receptors including fluorescent (Etayash et al., 2016), electrochemical (Adkins et al., 2017) and piezoelectric techniques (Han et al., 2018). Among various biomarkers, 16S ribosomal RNA (16S rRNA) is ideal for bacterium detection due to the high abundance (10^3–10^4 per actively growing cell) (Fu et al., 2016; Rogacs et al., 2012), ubiquity, evolutionary properties (which differ from mRNA and tRNA), and strong co-relationship with microbial activity (which unlike stable DNA, and solved false-negative detection problem caused by VBNC in culture method) (Case et al., 2007). The most common used 16S rRNA-based technique is 16S rRNA gene sequencing, it detect bacterium by sequencing full-length 16S rRNA and comparing with sequence data in database. (HirawatiKatoch, Chauhan, Singh, Sharma, Singh, Kashyap, Katoch) 16S rRNA gene sequencing method requires skilled personnel, high cost and long period to sequencing the full-length 16S rRNA, resulting to the fact that this technique could only performed in gene-sequencing companies and laboratories. Consequently, bacterium detection method with super-sensitivity, fast-response and capability to judge the microbial activity is still lacking and remains a major unmet need.

Among various signal receptors, electrochemical detection systems have the potential to achieve rapid and low-cost detection (Chen et al., 2016; Xiong et al., 2017; Lu et al., 2012). In order to obtain higher detection sensitivity, multichannel series piezoelectric quartz crystal (MSPQC) sensors which are based on the changes of electrical parameters are presented and widely used in clinical diagnosis (Guo et al., 2012; Battal et al., 2018; Yang et al., 2015). Our team reported a series of MSPQC sensors culture method-based strategy to achieve rapid detection of viable cell (He et al., 2016; Lian et al., 2015; Tong et al., 2014). The detection mechanisms of the previous works are based on the electric parameter change of culture medium which caused by the

* Corresponding author.
E-mail address: fengjiaohe@hnu.edu.cn (F. He).

https://doi.org/10.1016/j.bios.2019.05.007
Received 24 October 2018; Received in revised form 25 April 2019; Accepted 3 May 2019
Available online 06 May 2019
0956-5663/

metabolic products formed in cell growth. Although the detection time of previous proposed MSPQC sensors was shortened compared with other culture method-based strategy, the demand of early tests is still unmet owing to the limitation of bacterium generation time. Therefore, it is crucial to further shorten the time and improve the sensitivity in the development of advanced MSPQC sensor.

Silver staining is the general technology in electrophoresis to detect protein and gene by silver deposition on target (Zhang et al., 2007; Merril, 1987). Some researchers demonstrated the use of silver staining in EIS system to realize the highly sensitive DNA detection based on forming gene-templated metal wires between a pair of electrodes (Braun et al., 1998; Porath et al., 2000; Russell et al., 2014). Inspired by these works, we consider to introduce silver staining technology into MSPQC.

Herein, a supersensitive MSPQC sensor for bacterium detection was constructed. To demonstrate the feasibility of this sensor, a proof-of-concept method for *Escherichia coli* (*E. coli*) was designed and it exhibited ultra-sensitivity (LOD down to 2 cfu/mL), high specificity and rapid response in 2 h. More importantly, due to the use of 16S rRNA fragment as biomarker, the constructed sensor demonstrated strong correlation with bacterial activity. This potent MSPQC sensor can serve as a universal detection platform for super-sensitive detection of active bacterium, which might have great impact in the fields of public safety and early diagnosis.

2. Experimental section

2.1. Materials and equipment

All oligonucleotides, buffers, Spin Column Bacteria Total RNA Purification Kit and Total RNA Extractor (Trizol) are purchased from Sangon (Shanghai, China). All enzymes, adenosine 5′-triphosphate solution, dNTP mixture and tris-(2-carboxyethyl)-phosphine hydrochloride (TCEP) are purchased from BBI.

All used oligonucleotide sequences are listed in Table 1, and all thiol modified oligonucleotides are reduced by incubating with 0.1 M TCEP in 0.18 M phosphate buffer pH 8 for 1 h.

Gold electrode pair was composed of two gold electrodes and SiO_2 base as shown in Figure S-1. The electrodes are 2 mm long and 3 mm wide, the gap between two electrodes was 20 μm. The SiO_2 base is 10 mm long and 6 mm wide. 100 nm thick gold electrodes were contacted to SiO_2 base through 10 nm cadmium layer as shown in Figure S-2.

2.2. Preparation of bacterium MSPQC sensor

AuNPs-detection probe and detection cell were prepared to construct the presented sensor. Gold nanoparticles (14 nm) were prepared according to a standard citrate method (FRENS, 1973). AuNPs-detection probe was prepared by following procedure: 15 μL of 100 μM reduced oligonucleotides was mixed with 500 μL AuNPs solution and incubated for 12 h at 4 °C 50 μL 0.5 M NaCl solution was added and aged for 12 h. Excess NaCl was removed by centrifugation at 12,000 rpm for 25 min. The wine red precipitation represented the formation of AuNPs-oligonucleotides complex. Obtained complex was washed 3 times with 0.01 M phosphate buffer solution (pH 7.4) by centrifugation and then resuspended in 0.5 mL hybridization buffer for future use. Au NPs (2 nm)-detection probe was prepared using traditional method (Lee et al., 2008), Au NPs (50 nm)-detection probe and Au NPs (150 nm)-detection probe were synthesized according to Mirkin's method (Hurst et al., 2008).

Detection cell is composed of a pair of gold electrodes which modified with capture probe and hook probe on separated electrode surface. Gold electrode pair was treated with warm Piranha solution (30% H_2O_2 and 70% concentrated sulfuric acid) for 10 s, ultrasonically cleaned with ethanol and acetone for 5 min orderly, then rinsed with double-distilled water and dried for use. 1 μM reduced capture probe and hook probe were modified to electrode pair separately according to Braun's method (Braun et al., 1998). Both probes were self-assembled on the gold electrodes by incubated with 1 μM mercaptoethanol (MCH) overnight at 4 °C in 10 mM phosphate buffer (pH 8). The electrode pair was washed with 0.1 × SSC, dried and ready for use.

2.3. The detection procedure

2.3.1. Rolling circle amplification on electrodes

The hybridization and ligation of padlock probes were achieved by incubating 100 nM of the padlock probe with modified gold electrode, biomarker, 1 mM ATP, 0.2 μg/μL BSA and 0.05 U/μL T4 DNA ligase in 1 × ligation buffer for 1 h at 37 °C, thereafter the electrode pair was rinsed with 1 × TNT buffer and 0.1 × SSC. Rolling circle amplification is performed for 1 h at 37 °C using RCA reagent kit containing 1 × phi29 buffer, 0.25 mM dNTP, 0.2 μg/μL BSA, and 0.2 U/μL phi29 polymerase. The electrode pair was then washed by 0.1 × TNT and 0.1% SDS in sequence, subsequently dried by airflow.

2.3.2. Formation of silver wires along RCPs

50 nM detection probes were added in detection cell and bound to electrode pair by hybridization with RCPs at 37 °C for 1 h in 2 × SSC hybridization buffer. Uncombined probes were removed by washing with 0.1 × TNT and 0.1% SDS. The electrode pair was dried by airflow. Silver staining kit containing 0.2 M $AgNO_3$ solution and 0.1 M hydroquinone solution (pH = 10.5, adjusted by ammonium hydroxide) were added in detection cell, and stand for 10 min. Then 0.1 M $AgNO_3$ and 0.05 M hydroquinone (pH = 3.5, citrate buffer) were added orderly under low light conditions to form silver wires along RCPs.

2.4. Detection of E. coli

Total RNA was extracted from 1.5 mL, 1.0×10^5 cfu/mL *E. coli* using Total RNA Extractor (Trizol) according to the manufacturer's protocol. Extracted total RNA was then purified using the Spin Column Bacteria Total RNA Purification Kit (Trizol) to remove residual dNTP, NTP, and PPi. After column purification, RNA concentrations were determined using UV spectrophotometry, and the total RNA extracts were stored at −80 °C for future use. Total RNA were added into detection cell to initiate RNA on electrodes as shown in 2.3.1, followed by the formation of silver wires as described in 2.3.2.

Table 1
Oligonucleotide sequences used.

Function	Sequence
Biomarker	5′ GACCTTCGGGCCTCTTGCCATCGGATGTGCCCAGATGGGATTAGCTNGTNGGTGGGGTAACGGCTCACCTAGGCGACGATCCCTAGCTGGTCTGAGA GGATGACCAGCCACACTGGAACTGAGACACG-3′
Capture probe	5′HS-tctctctctctctctctctcTCCGATGGCAAGAGGCCCGAAGGTC-3′
Padlock probe	5′GTGTGGCTGGTCAGAAGAGTGTACCGACCTCTCGTCGAAGTAGCCGTGACTATCGACTtgcgtctatttagtggagccCGTGTCTCAGTTCCA-3
Detection probe	5′–HS–tgcgtctatttagtggagcc-3′
Hook probe	5′HS-tctctctctctctctctctcCGTCGAAGTAGCCGTGACTATCGAC-3′

2.5. Detection of E. coli in authentic sample

The bacterial lysis and preconditioning of sample were finished by adding Spin Column Bacteria Total RNA Purification Kit and Total RNA Extractor (Trizol). By simply adding corresponding regent kit (described in 2.3), RCA and silver staining were finished. The frequency shift is measured using $\Delta F = 32.80 \log_{10}C + 1430.537$, $R^2 = 0.989$, where C represents the concentration of *E. coli*.

2.6. Characterization of RCA in solution

Padlock probe and primer were denatured in 95 °C for 5min and placed in 4 °C before ligation. The reaction system for ligation is listed below: 100 nM padlock, target, 0.5 U//μL T4 DNA ligase in 1 × ligation buffer for 1 h at 22 °C, after that, solution was heated to 65 °C for 10 min to inactivate the enzyme. In order to degrade excess component (including linear padlock probe, unhybridized target and probe), the digestion was proceed before polymerization. Ligation products were added into digestion mixture solution (10 U/μL Exonuclease I, 5 U/μL Exonuclease III, 1 x Exonuelease I buffer, 1 x Exonuelease III buffer) in 37 °C for 2.5 h, and 95 °C for 20 min to inactivate enzyme. Rolling circle amplification was performed for 1 h at 30 °C using 1 × phi29 buffer, 0.2 mM dNTP, and 0.2 U/μL phi29 polymerase, and then heated to 65 °C for 10 min to inactivate enzyme.

3. Results and discussion

3.1. The constructive strategy of E. coli MSPQC sensor

The strategy of proposed method was shown in Scheme 1. A representative 16S rRNA fragment of specific region was used as biomarker of bacterium. The sequence of Capture probe is complementary to biomarker, and the sequence of hook probe is consistent of the stem part of padlock probe, both probes were immobilized on two separated gold electrodes respectively. 2-Mercaptoethanol (MCH) was used as blocker to prevent non-specific binding of nucleic acids (Liu et al., 2011). With the hybridization with capture probe, biomarker was bound on the electrode surface to initiate rolling circle amplification (RCA). In the presence of T4 ligase, padlock probe was ligated to the biomarker in a head-to-tail fashion, owing to the hybridization of biomarker and padlock probe (padlock probe consisted of "recognition region" and "signaling region", the sequence of "recognition region" is complementary to biomarker). In the presence of phi29 polymerase, RCAwas performed, leading to the formation of long single-strand RNA-DNA products containing repeated DNA-sequence units. Washed by anionic surfactant SDS in TNT buffer, the amplified products (RCPs) were ranged from one electrode surface to another, and bound to the opposite electrode surface by hybridizing with hook probe, resulting in the formation of linkage between two electrodes. Such linkage was called "gene link", it was non-conductive due to the electrical properties of long strand nucleic acids. In order to facilitate the formation of conductive metallic link between two electrodes, 14 nm oligonucleotides (detection probe)-functionalized AuNPs were assembled along RCPs. AuNPs were used as nucleation sites in further metallization. With the aid of AuNPs-DNA conjugates, the conductive "silver link" between two electrodes was formed. The switch from insulated "gene link" to conductive "silver link" led to the significant electrical parameter change of electrodes, resulting in sensitive response of MSPQC. In the absence of target, the electrodes remained non-conductive, while in the presence of target, the electrodes became conductive, the target acted as switch in proposed mechanism, so this strategy was called "DNA-RNA switch".

3.2. The selection and design of MSPQC system

The selection and design of MSPQC system is also the key design of the proposed sensor. Piezoelectric sensor, due to its high sensitivity, rapid processing, easy operation and low cost, has attracted more and more interest of the researchers (Han et al., 2018; El Kacimi et al., 2018; Zhao et al., 2018). Based on the contact mode between electrode and quartz crystal, piezoelectric sensor was classified into three types including normal piezoelectric quartz crystal (PQC), of which two electrodes were coated on quartz crystal; electrode-separated piezoelectric quartz crystal (ESPQC), of which quartz crystal was in the middle of two electrodes; and SPQC, where quartz crystal was connected in series with two electrodes. PQC and ESPQC could response to the mass change of quartz crystal surface, electric parameter, density and viscosity changes between two electrodes (Shen et al., 1993; Nomura et al., 1993). SPQC could only response to electric parameter change on electrode surface and medium between electrodes. As quartz crystal was sealed in metal box, the quality factor of crystal remained constant and the steady oscillation of quartz crystal could achieved (Yao et al., 1994). Multichannel was designed to realize the simultaneous detection of multiple samples using SPQC. MSPQC was selected as single detector and high-throughput detection was achieved.

The MSPQC system designed and made in our laboratory consisted of three sections: (I) data processing system, (II) detection cell system, and (III) oscillation circuit detection system, as shown in Fig. 1. The detection cell system included a pair of gold electrodes which connected in series with 9.0-MHz AT-cut quartz crystal. The detection cell was designed as detachable element, and the detection electrode was disposable in order to ensure the detection accuracy, which met the standard of medical test. By simply changing the detection electrode where loaded in different probes, the multiple bacteria detection could

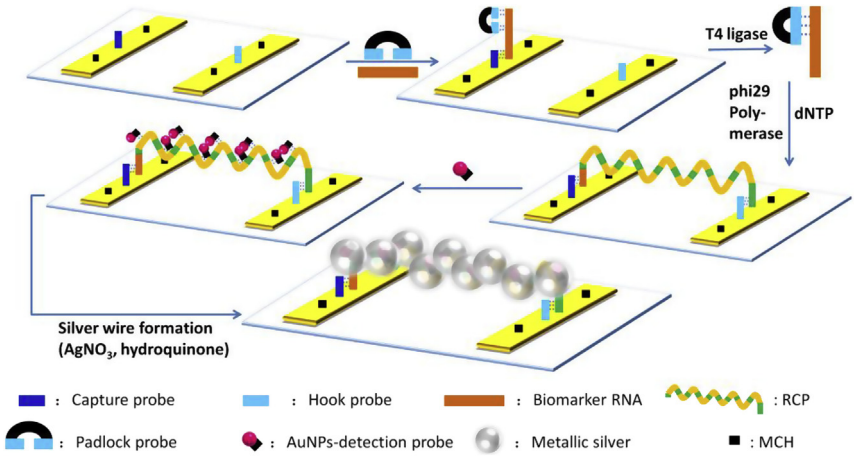

Scheme 1. The strategy of the supersensitive MSPQC sensor of bacterium based on 16S rRNA and "DNA-RNA switch".

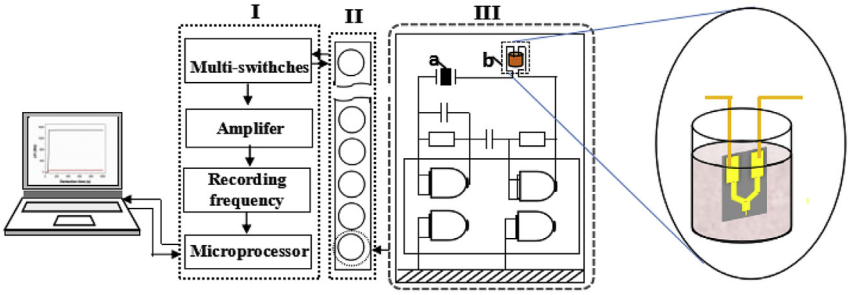

Fig. 1. Schematic of MSPQC sensor: (I) data acquisition device, (II) detection cell, (III) single oscillation circuit system.

be realized.

The response mechanism of MSPQC sensor to the electrical parameters changes can be expressed in Equation (1) (Shen et al., 1993):

$$\Delta F = \frac{\pi F_0^2 C_q (4\pi^2 F_0^2 C_s^2 Y + 4\pi F_0 C_s G - YG^2)}{[4\pi^2 F_0^2 C_s (C_0 + C_s) - 2\pi F_0 C_0 YG + G^2]^2} \cdot \Delta G \quad (1)$$

where:

ΔF is the frequency shift ($\Delta F = F_i - F_0$, and F_0 is the resonant frequency of the piezoelectric crystal).

C_q and C_O are motional capacitance and static capacitance of the crystal, respectively;

G and C_s are the conductance and capacitance of solution, respectively:

$G = \kappa\chi$, $C_s = \kappa\varepsilon + C_p$, ($\kappa$is the cell constant, x is the specific conductivity, ε is the solution permittivity and C_p is the parasitic capacitance between the leading wires of the electrodes);

$Y$is a parameter related to phase shift of the oscillator.

For the MSPQC used in this study, the frequency shift and the conductance change had a simple linear relationship in the range of 200–700 μS:

$$\Delta F = -k\Delta G$$

k is considered to be a constant, the value is different according to the shape of electrode, normally $k > 2$ (Mi et al., 2012; Tong et al., 2014).

3.3. The selection of the biomarker and designs of probes

Another key part of the proposed strategy is the selection of the biomarker and designs of probes. Using NCBI database, the sequence information of 16S rRNA was analysed, and the fragment of specific region was selected. The design principles and results of biomarker and probes were listed below:

Selection of biomarker: Since the specific regions of 16S rRNA reflect the differences among species, by choosing appropriate sequence in variable region as biomarker, the detection results could be consistent with that of using the entire 16S rRNA as biomarker (Welch and Huse, 2006). As a proof-of-concept, our strategy enabled the fast detection of *E. coli*. Fragment of region V1 was considered as biomarker of *E. coli* owing to the low intergenomic heterogeneity and high species specificity (Sundquist et al., 2007). The oligonucleotide sequences used are listed in Table 1.

The sequences of selected 16S rRNA fragment contain three parts: ①The red letters correspond to the sequences complementary to that of capture probe, which ensure the stable hybridization of biomarker and capture probe, the correctness of base-pairing and the specificity of proposed method; ② the blue letters correspond to the sequences complementary to that of "signaling region" of padlock probe, which ensure the specificity and efficiency of amplification; ③ the black letters are used to separate the binding regions of two probes, which reduce the tension and topological resistance, therefore insure the efficiency of RCA. Both terminal sequences of biomarker should be highly conserved in order to ensure effective hybridization.

Capture probe: The capture probe serves to immobilize the biomarker on one electrode of electrode pair. The lower–case letters were designed to reduce the non-specific adsorption of biomarker on electrode surface. The upper-case letters were the sequence complementary to that of biomarker.

Padlock probe: The padlock probe that consisted of "recognition region" (blue) and "signaling region" (green) was designed. Only when biomarker existed, a loop probe can be formed by hybridization between biomarker and the "recognition region" of padlock probe, then RCA can be performed.

Detection probes: 20 nt oligonucleotide which modified with gold nanoparticles was designed as detection probe, the oligonucleotide sequence was complementary to amplified products. A large number of AuNPs were assembled in the electrode gap by hybridization of detection probes with amplified products. The spacing between adjacent gold nanoparticles is affected by the length of detection probe. 20 nt sequences were designed in order to generate continuous silver wires.

Hook probe: Hook probe was modified to the opposite gold electrode by Au–S bonds in order to facilitate RCPs to span the gap of two electrodes. Lower-case letters represented sequences used to reduce non-specific binding on electrode surface, green upper-case letters represented sequences consistent with padlock probe.

3.4. Characterizations of detection process

The key factors of proposed sensor are the formation of RCA products (RCPs), the combination of RCPs and AuNPs, and silver staining. The formation of RCPs was further confirmed by the measurement of gel electrophoresis (Fig. 2 a.) and fluorescent spectra (figure S-3 in Supporting Information). As shown in Fig. 1, careful analysis of gel-electrophoresis figure reveals that the length of RCPs is far beyond 10000 nt (according to the comparison with marker), which ensure the feasibility of RCPs to bridge the gap between electrodes. Also, we accessed the efficiency of RCA by fluorescence spectra, the result is shown in Figure S-3. In order to realize the silver staining on RCPs, oligonucleotides functionalized AuNPs are prepared and hybridized with RCPs to guide the formation of silver wires. Transmission electron microscopy (TEM) figures of naked AuNPs (Fig. 2 b.) and AuNPs -DNA conjugates (Fig. 2 c.) reveal that in comparison of naked AuNPs, AuNPs-DNA complexes distribute more dispersed, and the outer layer of AuNPs are wrapped with a translucent and uniform layer (Fig. 2 d.), which indicates the formation of AuNPs-DNA complexes. The formation was further confirmed by the measurement of UV spectra and TEM, the results were shown in Figure S-4 (in Supporting Information). The hybridization reaction between RCPs and AuNPs-DNA was confirmed by TEM (Fig. 2 e.) and UV spectra (Figure S-5 in Supporting Information). TEM image reveals AuNPs-DNA complexes are arranged in line pattern, which resulting from the hybridization of RCPs and AuNPs-DNA complexes. The formation of silver nanowires which using amplified products as templates was characterized by AFM (Fig. 2 f.). By silver staining, the insulated gene link switched into conductive gene-

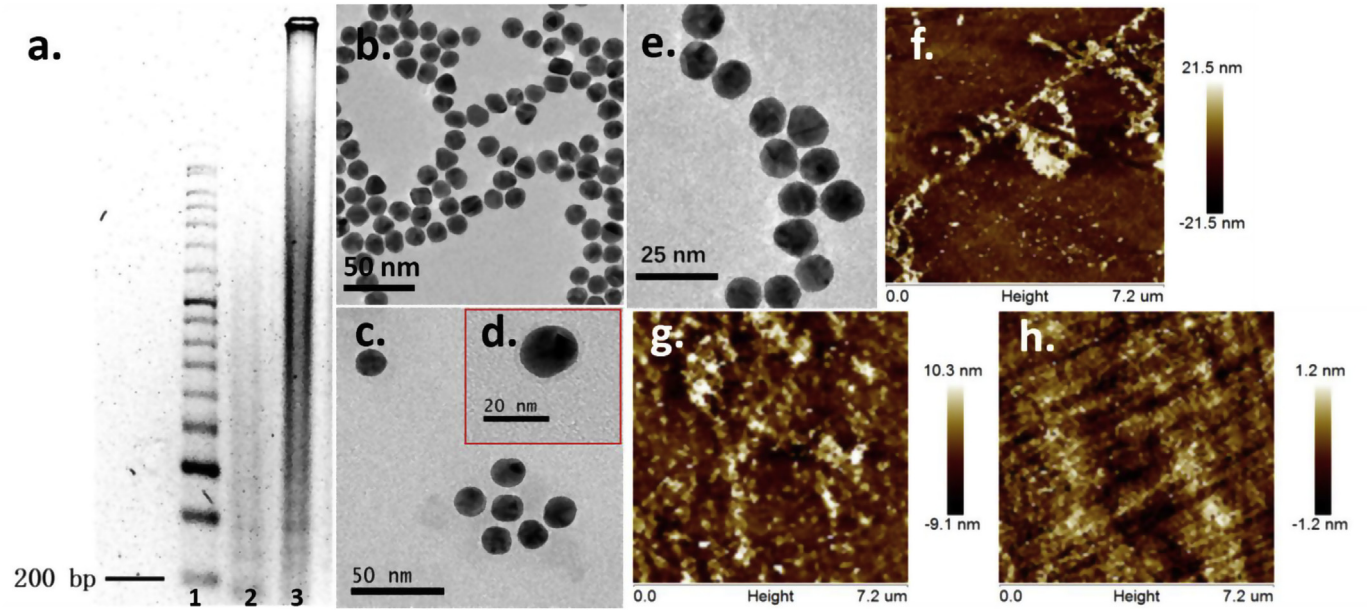

Fig. 2. (a.) Gel-electrophoresis figures of RCPs. Lanes 1–3 represent DNA ladder marker (200 bp), negative sample and positive sample, respectively. (b.) TEM image of naked AuNPs. (c.) TEM image of AuNPs-DNA conjugates. (d.) High resolution TEM image of single AuNPs-DNA conjugates. (e.) TEM image of AuNPs-DNA conjugates hybridized with RCPs. (f.) AFM phase image of the positive sample after silver staining. The silver nanowire formed based on RCPs as templates. The silver wire width was about 500 nm. (g.) AFM phase image of the negative sample after silver staining. The formation of silver is randomly distributed due to the lack of the guidance of gold nanoparticles. (h.) AFM phase image of naked electrode surface. (For interpretation of the references to colour in this figure legend, the reader is referred to the Web version of this article.)

templated silver nanowire. Owing to the electric parameter change of detection electrode, the super-sensitive detection of bacterium can be achieved.

When the reaction was conducted in the absence of 16S rRNA fragment, there is no continuous silver nanowire observed (Fig. 2 g), and the distribution of silver is irregular and random owing to the lack of RCPs.

In order to ensure the morphology captured by the AFM is caused by silver deposition, the effect of the roughness of the electrode surface itself should be excluded. AFM phase image of electrode surface is relatively flat (see Fig. 2 h., average height: 0.5 nm), while the height of silver deposition is much larger than that of the electrode surface itself (Fig. 2 g., average height: 5 nm; Fig. 1. 2., average height: 10 nm). Thus, the roughness of the electrode surface does not affect the characterization of deposited silver.

3.5. Optimization of detection conditions

3.5.1. Effects of MCH

MCH has two functions: First, to block the active sites of unconjugated capture probes and hook probes on the surface of electrode pair, reduce the non-specific binding on the electrode (Chen et al., 2018). Second, owing to the electrostatic repulsion between the negative charge of relatively rigid MCH and DNA skeleton, the capture probes tend to keep upright and extend into solution, which facilitate the identification and hybridization of the biomarker. Therefore, the concentration of MCH could affect the detection performance of proposed sensor. The experimental results were shown in Table 2. With the increasing of the concentration of MCH from 1 μM to 50 μM, the frequency change ΔF (ΔF = F – F_0, where F_0 and F are the frequency in the absence and presence of *E. coli* with concentration at 10^5 cfu/mL) decreased. 1 μM MCH was chosen for optimal concentration.

3.5.2. Optimization of silver staining conditions

The effect of the concentration of the developer solution (in terms of $AgNO_3$) is also discussed and shown in Fig. 3. With the increasing of the concentration of $AgNO_3$ from 0.01 M to 0.3 M, ΔF keeps increased. When it reached 0.2 M, ΔF reached a plateau. Thus, 0.2 M $AgNO_3$ was chosen for metallization of RCPs.

Table 2
The effect of MCH concentration on frequency response.

Concentration (μM)	Frequency change (× 10^3 Hz)	RSD (%, n = 3)
0.5	1.51	4.0
1	1.59	2.9
2	1.58	1.8
5	1.55	5.4
10	1.43	4.5
50	1.04	3.8

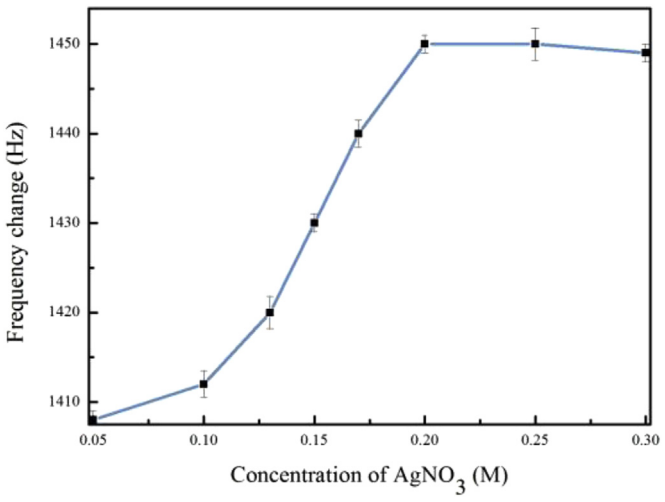

Fig. 3. The effect of $AgNO_3$ concentration on frequency response.

Table 3
The effect of AuNPs particle size on frequency response.

Diameter (nm)	Frequency change (× 10^3 Hz)	RSD (%, n = 3)
2	1.27	5.5
14	1.51	2.9
50	1.51	5.1
150	1.50	3.6

3.5.3. Optimization of particle size of Au NPs

The change of Au NPs particle size was also investigated (Table 3). To investigate the influence of the particle size of Au NPs, a diameter of 2 nm, 14 nm, 50 nm and 150 nm Au NPs were used, the TEM images of different size of Au NPs was shown in Figure S-6. As shown in Table 3, as the particle size of AuNPs increased, the frequency change increased gradually until 14 nm AuNPs was used. Though the radius of Au NPs was changed from 14 nm to 150 nm, there was little change in the frequency change. In order to obtain optimal detection sensitivity and easy operation, 14 nm Au NPs was selected.

3.6. Detection of E. coli

3.6.1. Quantitative detection of E. coli

Upon optimum conditions, the quantitative detection of *E. coli* based on the MSPQC sensor was tested. 1 μM MCH and 0.2 M $AgNO_3$ were chosen for optimal concentration. The frequency-time response curves for varying concentration of *E. coli* (0~10^7 cfu/mL) were shown in Fig. 4A, and based on the data of the frequency-time response curves, the frequency-concentration calibration curve was analysed and shown in Fig. 4B, where Frequency change = F – F_0, F_0 and F are the frequency in the absence and presence of *E. coli*. It can be seen that ΔF showed linear relationship with the logarithm of *E. coli* from concentration in range of 10 to 10^7 cfu/mL, i.e. $\Delta F = 32.80 \log_{10}C + 1430.537$, $R^2 = 0.989$, where C represents the concentration of *E. coli*. The detection limit (LOD) is 2 cfu/mL, it was determined by the equation LOD = 3 × (SD/k), where SD is the standard deviation of the measurement signal for the blank sample, and k is the slope of the analytical curve in the linear region.

3.6.2. Selectivity study of proposed sensor

The selectivity of our proposed method to *E. coli* was studied by detecting other pathogens like *Salmonella enteritidis*, *Staphylococcus aureus*, *Listeria innocua*, and *Pseudomonas aeruginosa*. The concentrations of four pathogens were 1.0 × 10^5 cfu/mL. The mixture sample (1.0 × 10^5 cfu/mL *E. coli* + 1.0 × 10^5 cfu/mL other four pathogens) was also detected by proposed method. The results were shown in

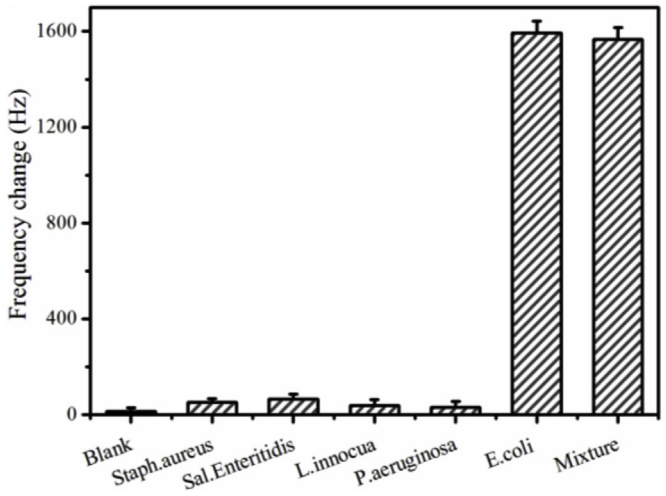

Fig. 5. Selectivity study for *E. coli*.

Fig. 5. The degree of interference (DI) of these four pathogens to *E. coli* can be evaluated using following equation:

$$DI = \triangle F_I / \triangle F_E \times 100\%$$

Where $\triangle.F_I$ and $\triangle.F_E$ were corresponding to the frequency resulted by four interfering pathogens and *E. coli*. DI values for *Staphylococcus aureus*, *Salmonella enteritidis*, *Listeria innocua* and *Pseudomonas aeruginosa* were calculated as 0.942%, 1.30%, 0.98% and 1.03%, respectively. These mean that the interference of these four pathogens could be negligible. The frequency of mixture showed only a slight change of 0.40% compared to the sample containing only *E. coli*, indicating that there was no cross-reactivity with four interfering pathogens in constructed sensor. The above results revealed the ultra-high sensitivity and high specificity of the proposed method.

3.6.3. Detection of E. coli in authentic sample

In order to access the applicability of proposed method for *E. coli* detection in real samples, simulated human serum and milk sample was prepared by incorporating *E. coli* at different target concentrations from 10 cfu/mL to 10^7 cfu/mL. The results in Table 4 show that the recoveries varied from 99.00% to 107.00%,which indicate the applicability of proposed method for detection of *E. coli* in simulated samples. Besides, the limit of detections in the human serum and milk sample for *E. coli* are both 10 cfu/mL. Moreover, the detection only takes 2 h to detect *E. coli*, which typically takes 48 h or even more by culture method, indicating that the proposed method could be used to detect *E.*

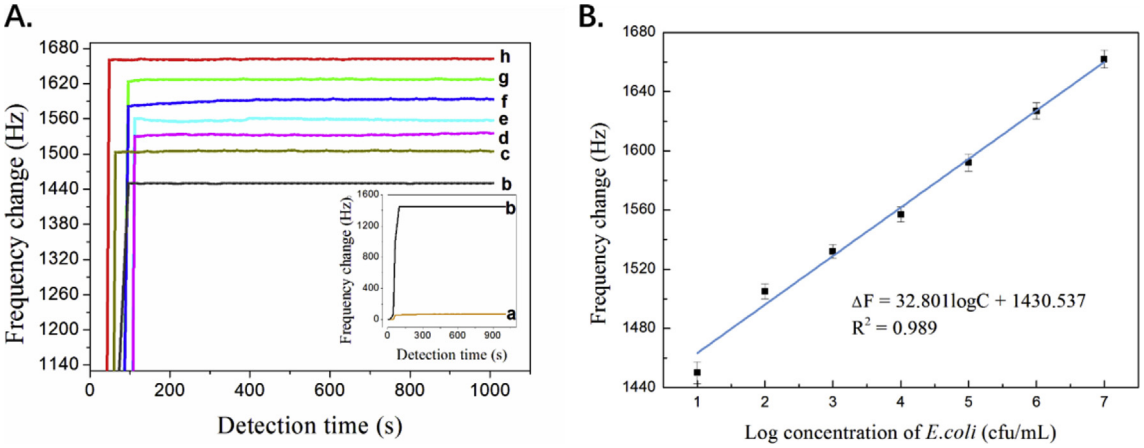

Fig. 4. A. Frequency-time response curves for different concentrations of *E. coli* (curves a–g correspond to 0, 10, 10^2, 10^3, 10^4, 10^5, 10^6 and 10^7 cfu/mL, respectively). B. Calibration curve for the frequency change of *E. coli* in different concentration (logarithmic scale). Error bars indicate standard deviation (n = 3).

Table 4
Recovery efficiency of *E.coli* detected in real samples based on the proposed sensor.

Samples	Added ($\log_{10} N$ cfu/mL)	Measured ($\log_{10} N$ cfu/mL)	Recovery (%)	RSD (%, $n = 3$)
Human serum 1	1	1.01	101.00	7.48
Human serum 2	3	2.98	99.33	5.04
Human serum 3	5	5.11	102.20	2.37
Human serum 4	7	6.98	99.71	3.88
Milk 1	1	1.02	102.00	5.98
Milk 2	3	3.21	107.00	4.30
Milk 3	5	4.96	99.20	2.81
Milk 4	7	7.10	101.43	1.37

coli rapidly and sensitively in real sample.

4. Conclusion

Our detection method is compared with the recently published work on bacterium detection, as shown in Tables S–1. Compared with culture method, our proposed detection method is rapid, capable of detecting VBNC bacteria. Compared with DNA-based and mRNA-based strategy, proposed method is sensitive, specific and could achieve microbial activity testing. In comparison to previous MSPQC sensor, proposed sensor exhibits super-sensitive owing to the introduction of "DNA-RNA switch". Besides, due to the structural characteristic of 16S rRNA (wide distribution and relative variability), our proposed method might construct a sensitive and universal bacterium detection platform.

CRediT authorship contribution statement

Ye Feng: Conceptualization, Methodology, Formal analysis, Investigation, Writing - original draft. **Xiaoqing Zhang:** Software, Methodology, Investigation. **Lingling Su:** Data curation, Formal analysis. **Yilin Zhang:** Validation, Software. **Fengjiao He:** Resources, Writing - original draft, Visualization, Supervision, Project administration, Funding acquisition.

Acknowledgment

This research work was supported by a grant from the National Natural Science Foundation of China (No. 21275042); Hunan Provincial Science and Technology Department (No. 2015JC3072).

Appendix A. Supplementary data

Supplementary data to this article can be found online at https://doi.org/10.1016/j.bios.2019.05.007.

References

Adkins, J.A., Boehle, K., Friend, C., Chamberlain, B., Bisha, B., Henry, C.S., 2017. Colorimetric and electrochemical bacteria detection using printed paper- and transparency-based analytic devices. Anal. Chem. 89 (6), 3613–3621. https://doi.org/10.1021/acs.analchem.6b05009.

Battal, D., Akgönüllü, S., Yalcin, M.S., Yavuz, H., Denizli, A., 2018. Molecularly imprinted polymer based quartz crystal microbalance sensor system for sensitive and label-free detection of synthetic cannabinoids in urine. Biosens. Bioelectron. 111, 10–17. https://doi.org/https://doi.org/10.1016/j.bios.2018.03.055.

Braun, E., Eichen, Y., Sivan, U., Ben-Yoseph, G., 1998. DNA-templated assembly and electrode attachment of a conducting silver wire. Nature 391 (6669), 775–778. https://doi.org/10.1038/35826.

Case, R.J., Boucher, Y., Dahllöf, I., Holmström, C., Doolittle, W.F., Kjelleberg, S., 2007. Use of 16S RRNA and RpoB genes as molecular markers for microbial ecology studies. Appl. Environ. Microbiol. 73 (1), 278–288. https://doi.org/10.1128/AEM.01177-06.

Chen, T., Liu, D., Lu, W., Wang, K., Du, G., Asiri, A.M., Sun, X., 2016. Three-dimensional Ni2P nanoarray: an efficient catalyst electrode for sensitive and selective nonenzymatic glucose sensing with high specificity. Anal. Chem. 88 (16), 7885–7889. https://doi.org/10.1021/acs.analchem.6b02216.

Chen, S., Chen, Q., Li, Q., An, J., Sun, P., Ma, J., Gao, H., 2018. Biodegradable synthetic antimicrobial with aggregation-induced emissive luminogens for temporal antibacterial activity and facile bacteria detection. Chem. Mater. 30 (5), 1782–1790. https://doi.org/10.1021/acs.chemmater.8b00251.

El Kacimi, A., Pauliac-Vaujour, E., Eymery, J., 2018. Flexible capacitive piezoelectric sensor with vertically aligned ultralong GaN wires. ACS Appl. Mater. Interfaces 10 (5), 4794–4800. https://doi.org/10.1021/acsami.7b15649.

Etayash, H., Khan, M.F., Kaur, K., Thundat, T., 2016. Microfluidic cantilever detects bacteria and measures their susceptibility to antibiotics in small confined volumes. Nat. Commun. 7, 1–9. https://doi.org/10.1038/ncomms12947.

FRENS, G., 1973. Controlled nucleation for the regulation of the particle size in monodisperse gold suspensions. Nat. Phys. Sci. (Lond.) 241 (105), 20–22. https://doi.org/10.1038/physci241020a0.

Fu, Y., Chen, H., Liu, L., Huang, Y., 2016. Single cell total RNA sequencing through isothermal amplification in picoliter-droplet emulsion. Anal. Chem. 88 (22), 10795–10799. https://doi.org/10.1021/acs.analchem.6b02581.

Gayathri, C.H., Mayuri, P., Sankaran, K., Kumar, A.S., 2016. An electrochemical immunosensor for efficient detection of uropathogenic E. Coli based on thionine dye immobilized chitosan/functionalized-MWCNT modified electrode. Biosens. Bioelectron. 82, 71–77. https://doi.org/10.1016/j.bios.2016.03.062.

Guo, X., Lin, C.S., Chen, S.H., Ye, R., Wu, V.C.H., 2012. A piezoelectric immunosensor for specific capture and enrichment of viable pathogens by quartz crystal microbalance sensor, followed by detection with antibody-functionalized gold nanoparticles. Biosens. Bioelectron. 38 (1), 177–183. https://doi.org/10.1016/j.bios.2012.05.024.

Han, J., Tong, F., Chen, P., Zeng, X., Duan, Z., 2018. Study of inflammatory factors' effect on the endothelial barrier using piezoelectric biosensor. Biosens. Bioelectron. 109 (February), 43–49. https://doi.org/10.1016/j.bios.2018.02.064.

He, F., Xiong, Y., Liu, J., Tong, F., Yan, D., 2016. Construction of Au-IDE/CFP10-ESAT6 aptamer/DNA-AuNPs MSPQC for rapid detection of Mycobacterium Tuberculosis. Biosens. Bioelectron. 77, 799–804. https://doi.org/10.1016/j.bios.2015.10.054.

Hirawati, Katoch, K., Chauhan, D.S., Singh, H.B., Sharma, V.D., Singh, M., Kashyap, M., Katoch, V.M., 2006HirawatiKatoch, Chauhan, Singh, Sharma, Singh, Kashyap, Katoch. Detection of M. Leprae by reverse transcription- PCR in biopsy specimens from leprosy cases: a preliminary study. J. Commun. Dis. *38* (0019–5138), 280–287 (Print)).

Hurst, S.J., Hill, H.D., Mirkin, C.A., 2008. "Three-Dimensional hybridization" with polyvalent DNA − Gold nanoparticle conjugates. J. Am. Chem. Soc. 130 (36), 12192–12200. https://doi.org/10.1021/ja804266j.

Lee, J.-S., Seferos, D.S., Giljohann, D.A., Mirkin, C.A., 2008. Thermodynamically controlled separation of polyvalent 2-nm gold nanoparticle-oligonucleotide conjugates. J. Am. Chem. Soc. 130 (16), 5430–5431. https://doi.org/10.1021/ja800797h.

Lian, Y., He, F., Wang, H., Tong, F., 2015. A new aptamer/graphene interdigitated gold electrode piezoelectric sensor for rapid and specific detection of Staphylococcus aureus. Biosens. Bioelectron. 65, 314–319. https://doi.org/10.1016/j.bios.2014.10.017.

Liu, Z., Zhang, W., Zhu, S., Zhang, L., Hu, L., Parveen, S., Xu, G., 2011. Ultrasensitive signal-on DNA biosensor based on nicking endonuclease assisted electrochemistry signal amplification. Biosens. Bioelectron. 29 (1), 215–218. https://doi.org/10.1016/j.bios.2011.07.076.

Lu, W., Qin, X., Liu, S., Chang, G., Zhang, Y., Luo, Y., Asiri, A.M., Al-Youbi, A.O., Sun, X., 2012. Economical, green synthesis of fluorescent carbon nanoparticles and their use as probes for sensitive and selective detection of mercury(II) ions. Anal. Chem. 84 (12), 5351–5357. https://doi.org/10.1021/ac3007939.

Merril, C.R., 1987. Silver-stain detection of proteins separated by polyacrylamide gel electrophoresis. In: *ACS Symposium Series*; ACS Symposium Series. vol. 335. American Chemical Society, pp. 5–74. https://doi.org/doi:10.1021/bk-1987-0335.ch005.

Mi, X., He, F., Xiang, M., Lian, Y., Yi, S., 2012. Novel phage amplified multichannel series piezoelectric quartz crystal sensor for rapid and sensitive detection of Mycobacterium Tuberculosis. Anal. Chem. 84 (2), 939–946. https://doi.org/10.1021/ac2020728.

Nomura, T., Ohno, Y., Takaji, Y., 1993. Single drop method for determination of ions using an electrodeless piezoelectric quartz crystal. Anal. Chim. Acta 272 (2), 187–192. https://doi.org/https://doi.org/10.1016/0003-2670(93)80568-6.

Porath, D., Bezryadin, A., de Vries, S., Dekker, C., 2000. Direct measurement of electrical transport through DNA molecules. Nature 403, 635.

Rogacs, A., Qu, Y., Santiago, J.G., 2012. Bacterial RNA extraction and purification from whole human blood using isotachophoresis. Anal. Chem. 84 (14), 5858–5863. https://doi.org/10.1021/ac301021d.

Russell, C., Welch, K., Jarvius, J., Cai, Y., Brucas, R., Nikolajeff, F., Al, R.E.T., 2014. Gold nanowire based electrical DNA detection using rolling circle ampli fi cation. ACS Nano 8, 1147–1153. https://doi.org/10.1021/nn4058825.

Shen, D.Z., Zhu, W.H., Nie, L.H., Yao, S.Z., 1993. Behaviour of a series piezoelectric sensor in electrolyte solution: Part I. Theory. Anal. Chim. Acta 276 (1), 87–97.

https://doi.org/https://doi.org/10.1016/0003-2670(93)85042-I.
Sun, Y., Zhao, C., Yan, Z., Ren, J., Qu, X., 2016. Simple and sensitive microbial pathogen detection using a label-free DNA amplification assay. Chem. Commun. 52 (47), 7505–7508. https://doi.org/10.1039/C6CC02672A.
Sundquist, A., Bigdeli, S., Jalili, R., Druzin, M.L., Waller, S., Pullen, K.M., El-Sayed, Y.Y., Taslimi, M.M., Batzoglou, S., Ronaghi, M., 2007. Bacterial flora-typing with targeted, chip-based pyrosequencing. BMC Microbiol. 7, 1–11. https://doi.org/10.1186/1471-2180-7-108.
Tong, F., Lian, Y., Zhou, H., Shi, X., He, F., 2014. Multichannel series piezoelectric quartz crystal cell sensor for real time and quantitative monitoring of the living cell and assessment of cytotoxicity. Anal. Chem. 86 (20), 10415–10421. https://doi.org/10.1021/ac502926k.
Welch, D.B.M., Huse, S.M., 2006. Microbial diversity in the deep sea and the under-explored “rare biosphere.”. Proc. Natl. Acad. Sci. Unit. States Am. 103, 12115–12120. https://doi.org/10.1002/9781118010549.ch24.
Xiong, X., You, C., Cao, X., Pang, L., Kong, R., Sun, X., 2017. Ni2P nanosheets array as a novel electrochemical catalyst electrode for non-enzymatic H2O2 sensing. Electrochim. Acta 253, 517–521. https://doi.org/https://doi.org/10.1016/j.electacta.2017.09.104.
Yang, Z., Liu, X., Zhang, C., Liu, B., 2015. A high-performance nonenzymatic piezoelectric sensor based on molecularly imprinted transparent TiO2 film for detection of urea. Biosens. Bioelectron. 74, 85–90. https://doi.org/https://doi.org/10.1016/j.bios.2015.06.022.
Yao, S., Chen, K., Zhu, F., Shen, D., Nie, L., 1994. Surface acoustic wave sensor system for the determination of total salt content in serum. Anal. Chim. Acta 287 (1), 65–73. https://doi.org/https://doi.org/10.1016/0003-2670(94)85102-6.
Yu, F., Li, Y., Li, M., Tang, L., He, J.J., 2017. DNAzyme-integrated plasmonic nanosensor for bacterial sample-to-answer detection. Biosens. Bioelectron. 89, 880–885. https://doi.org/10.1016/j.bios.2016.09.103.
Zhang, M., Wittstock, G., Shao, Y., Girault, H.H., 2007. Scanning electrochemical microscopy as a readout tool for protein electrophoresis. Anal. Chem. 79 (13), 4833–4839. https://doi.org/10.1021/ac062356k.
Zhang, X., Shen, J., Ma, H., Jiang, Y., Huang, C., Han, E., Yao, B., He, Y., 2016. Optimized dendrimer-encapsulated gold nanoparticles and enhanced carbon nanotube nanoprobes for amplified electrochemical immunoassay of E. Coli in dairy product based on enzymatically induced deposition of polyaniline. Biosens. Bioelectron. 80, 666–673. https://doi.org/10.1016/j.bios.2016.02.043.
Zhang, D., Bi, H., Liu, B., Qiao, L., 2018. Detection of pathogenic microorganisms by microfluidics based analytical methods. Anal. Chem. 90, 5512–5520. https://doi.org/10.1021/acs.analchem.8b00399.
Zhao, G., Zhang, X., Cui, X., Wang, S., Liu, Z., Deng, L., Qi, A., Qiao, X., Li, L., Pan, C., et al., 2018. Piezoelectric polyacrylonitrile nano fi ber film-based dual-function self-powered flexible sensor. ACS Appl. Mater. Interfaces 10 (18), 15855–15863. https://doi.org/10.1021/acsami.8b02564.
Zhou, C.-X., Mo, R.-J., Chen, Z.-M., Wang, J., Shen, G.-Z., Li, Y.-P., Quan, Q.-G., Liu, Y., Li, C.-Y., 2016. Quantitative label-free Listeria analysis based on aptamer modified nanoporous sensor. ACS Sens. 1 (8), 965–969. https://doi.org/10.1021/acssensors.6b00333.